Hardware-in-the-loop Experiments on an Active Turning Tool with Robust LPV Control of Chatter Vibration

Ziv Brand
Dept. Mechanical Engineering
Shamoon College of Engineering, SCE
Be'er Sheva, Israel
e-mail: zivbr@sce.ac.il

Matthew O.T. Cole
Dept. Mechanical Engineering
Chiang Mai University, CMU
Chiang Mai, Thailand
e-mail: motcole@dome.eng.cmu.ac.th

***Abstract*— This study presents a control design for an active lathe cutting tool aimed at effectively suppressing vibration and chatter during internal turning operations. To address the variability in dynamic behavior caused by uncertainties in cutting parameters, a robust H_∞ controller was developed using a Linear-Parameter-Varying (LPV) model of the machining dynamics. This parametric approach allows real-time tuning of the control system properties in a workshop environment for optimal vibration reduction. The controller manages time-delayed feedback from cutting forces and mitigates spillover instability from unmodeled high-frequency modes. Integrated with piezoelectric actuators and sensors, the active tool holder maintains its original size and shape, ensuring ease of use in industrial applications. Experiments using a laboratory system that emulates chatter showed that the proposed system reduces root-mean-square vibration levels by over 65%, with peak-to-peak values reduced by approximately 47% in unstable cutting regimes. These results demonstrate the system's feasibility for real-world machining environments, enabling higher material removal rates with improved surface finish.**

Keywords- Active vibration control; Chatter suppression; Internal turning; Linear parameter varying control; H-infinity control.

I. INTRODUCTION

Machining processes are crucial in the production of high-precision components, with the global machining market projected to reach approximately USD 100 billion by 2025, based on a Compound Annual Growth Rate (CAGR) of 7% between 2019 and 2025. CNC lathes represent around 20% of all machine tools, playing a significant role in modern manufacturing [1]. However, mechanical vibrations, particularly chatter, remain a persistent challenge in these processes. Chatter is a type of self-excited vibration that leads to poor surface finish quality, increased tool wear, and elevated noise levels. In Computer Numerical Control (CNC) lathes, avoiding chatter typically requires setting conservative values of machining parameters such as reduced cutting depth, slower spindle speeds, and decreased feed rates, all of which lower production efficiency [2].

Additionally, the avoidance of vibration problems in internal turning operations imposes limits on tool holder geometry. As the ratio between tool overhang and diameter (L/D, Length-to-Diameter ratio) increases, the stability margins decrease due to reduced bending stiffness [2]. This limitation restricts the length of standard tools, with current solutions ranging from L=4D to 14D depending on what materials and vibration control methods are used. For instance, the length of steel shank tools is limited to 4D, while solid carbide tools can reach 7D, and passive vibration-controlled tools can achieve up to 10D. Solid carbide tool shanks with passive control devices can reach up to 14D [3].

This study explores the significant potential of tool-integrated active vibration control to reduce chatter in internal turning. We focus on the development of a robust LPV feedback control system, which is demonstrated and evaluated through a laboratory emulator system. The experimental setup incorporates a piezoelectric actuator, and a PZT-type vibration sensor mounted to a standard turning tool. The goal is to create a control system that not only enhances vibration suppression but also allows the flexibility of on-the-job tuning to optimize performance according to the setup conditions.

Piezoelectric materials can operate as transducers in a dual manner: the direct piezoelectric effect involves the conversion of mechanical forces into electrical potential, while the inverse piezoelectric effect can convert an applied electric field into mechanical deformation of the material [4]. Piezoelectric components are widely used for active vibration suppression. Examples include vibration reduction of thin-walled rotors [5][6], cables [7], composite laminated plates [8], aerospace applications [9], and research for CNC lathes [10][11].

Various active control approaches for suppressing vibrations in cutting tool holders have been studied and are still actively being researched. These include the use of PID controllers [12], H-infinity state feedback control strategies [10], H-infinity controller design based on Linear Matrix Inequalities (LMI) [13], model-free finite frequency H_∞ control [11], and input shaping control [14], among others. The model-based design of a robust control algorithm for vibration suppression in the turning process presents many challenges. In this work, the effect of parametric uncertainties and time-delay feedback—both inherent in machining processes—are taken into consideration.

To address the uncertain dynamics, a robust parameter-dependent H_∞ controller is synthesized, where the robustness/gain properties can be adjusted in real-time within a workshop environment to achieve optimal vibration reduction, making it more practical in machining processes

subject to parametric uncertainty. The controller design considers uncertain time-delayed feedback effects from cutting forces and aims to prevent spillover instability of unmodeled and uncertain higher-order modes. Laboratory experiments conducted using a cutting emulation system demonstrate that the proposed approach can successfully transition the system from unstable to stable operation achieving a vibration reduction of approximately 65%.

Within the paper, Section II defines the dynamic model of the active tool system and presents the methodology for designing the robust H_∞ controller based on the LPV framework. Section III describes the experimental setup, followed by Section IV, which provides the practical evaluations and results from the turning emulation tests conducted in the laboratory. Section V concludes the paper with key findings and recommendations for future work.

II. DYNAMIC MODEL

This section presents the mathematical formulation and modeling approach used to describe the tool's dynamic response during internal turning operations.

A. Turning process model

The internal turning process involves dynamic interactions between the tool structure and the rotating workpiece at the material removal point. Modeling principles for these dynamics have been established in previous studies [15][16]. For practical approximation, the forced excitation of the tool can be effectively modeled using a single-degree-of-freedom dynamic representation that captures the dominant bending mode of the tool holder. With the inclusion of actuation force, a lumped mass model is found to be suitable:

$$m\ddot{x}(t) + c\dot{x}(t) + kx(t) = Ku(t) + f_c(t) \qquad (1)$$

where f_c represents the radial cutting force, u is the control input (voltage), and K is the coupling coefficient for the piezoelectric actuator. The parameters m, c and k denote the effective mass, damping, and stiffness of the dominant mode, respectively. Converting this expression into the Laplace domain gives:

$$X(s) = \Phi(s) \cdot \left(K_1 \cdot U(s) + K_2 \cdot F_c(s)\right) \qquad (2)$$

where $\Phi(s) = \frac{1}{s^2+2\zeta\omega_n s+\omega_n^2}$ with $\omega_n = \sqrt{k/m}$ being the natural frequency, and $\zeta = c/\left(2\sqrt{k/m}\right)$ the damping ratio. The static gains are $K_1 = K/m$ and $K_2 = 1/m$.

To predict chatter, the cutting force model must connect the time-varying tool deflection $x(t)$ to the instantaneous chip thickness $h(t)$ and corresponding cutting force $f_c(t)$. In longitudinal cutting, an overlap factor $\Psi = b_d/b$ is used to account for the influence of previous tool deflections on the current chip thickness [17]. This concept is illustrated in Figure 1 for a standard bull-nose end cutter. The effective chip width b is determined by the cutting-edge shape, while the overlap length b_d depends on the feed per revolution. For small radial deflections $x(t)$, the instantaneous chip thickness can be expressed as:

$$h(t) = h_m(t) - [x(t) - \Psi x(t-\tau)] \qquad (3)$$

where $h_m(t)$ is the mean chip thickness over the width of the cut, and τ is the time delay from one period of spindle rotation: $\tau = 60/\Omega$ where Ω is the rotational speed in rpm. The radial cutting force can be expressed

$$f_c(t) = f_{tr}(t)\cos\beta + C_s\frac{b}{V}\dot{x}(t), \qquad (4)$$

where $f_{tr}(t) = K_s b h(t)$ is the cutting force projected onto the $x-y$ plane, β is the angle between the cutting force and radial direction, C_s is the process damping, and $V = \pi d\Omega/60$ is the cutting velocity, where d is the workpiece diameter, and K_s is the specific cutting force appropriate to the material properties and cutting conditions. The turning process model is represented by the block diagram in Figure 2, where $e^{-\tau s}$ represents the time delay.

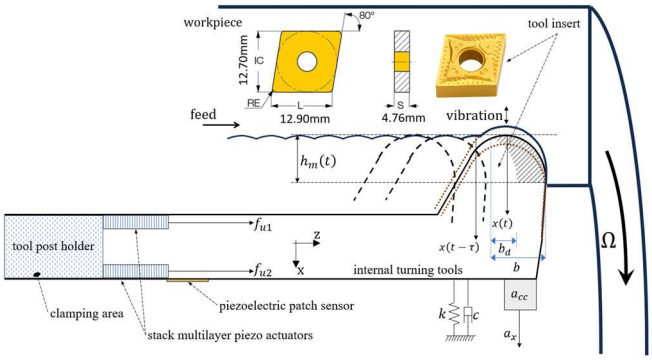

Figure 1. Schematic diagrams of internal turning process.

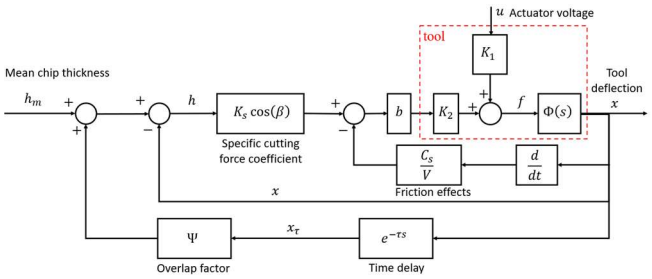

Figure 2. Turning process dynamics with active tool holder.

B. Robust stability and controller synthesis for cutting processes with delayed feedback

The optimization of the feedback control algorithm must balance high performance with avoiding excessive controller gain, which could lead to actuator voltage saturation, system instability, or noise amplification. Robust controller design must account for potential differences between the actual system dynamics $G_0(s)$ and the model transfer function $G(s)$. This can be represented by a multiplicative error factor $\Delta_m(s)$

such that $G_0 = G + \Delta_m G$. When a bound for Δ_m is known or estimated, the small gain theorem can be used to ensure stability and performance of the closed-loop system.

A key challenge is that model accuracy can vary depending on the tool setup, and precise determination of Δ_m, or its bounds, may not always be feasible. Additional uncertainty arises in the cutting force model due to factors like material hardness, cutting speed, and feed rate. Therefore, a systematic approach is needed to handle both model and cutting process uncertainties in the controller design.

The system dynamics for controller synthesis are depicted in Figure 3, where the multiplicative model error (Δ_m) and the time-delayed feedback block ($e^{-\tau s}$) are treated as uncertain external feedback loops. The lumped parameter $\kappa = K_2 K_s b \cos\beta / K_1$ is both uncertain and potentially time-varying, depending on the current cutting conditions. Designing a controller for the maximum expected value of κ may ensure suitability for the maximum depth of cut but could compromise robustness. Instead, a κ-dependent controller is proposed, which can be tuned online to match system setup and cutting conditions. This synthesis is done using the gain-scheduled H_∞ framework, which requires the plant model's state-space matrices to have an affine dependency on the parameters, i.e., be in LPV form. The parameter $\delta = C_s/(V \cos\beta\, K_s)$, representing process damping is also uncertain; however, designing the controller for the smallest value of δ is appropriate as larger values increase damping and improve stability.

The LPV control synthesis problem is defined by considering d and x_τ as exogenous inputs, and f and x as outputs, as shown in Figure 3. The impact of Δ_m and the delayed feedback ($e^{-\tau s}$) are handled using H_∞ norm-bound criteria for robust stability [18, 19]. Three design specifications are defined:

1. Robust Stability under Delayed Feedback:
$$\left\|T_{xx_\tau}(K_c,\kappa)\right\|_\infty < 1 \leftrightarrow \|\kappa T_{xd}(K_c,\kappa)\|_\infty < \Psi^{-1}.$$
2. Forced Disturbance Attenuation:
$$\left\|W_1 T_{xh_m}(K_c,\kappa)\right\|_\infty < 1 \leftrightarrow \|\kappa W_1 T_{xd}(K_c,\kappa)\|_\infty < 1,$$
where $W_1(s)$ is a weighting function representing the disturbance spectrum.
3. Robust Stability under Model Error (Δ_m):
$$\left\|\Delta_m T_{fd}(K_c,\kappa)\right\|_\infty < 1 \leftarrow \|W_2 T_{ud}(K_c,\kappa)\|_\infty < 1,$$
where $W_2(s)$ is chosen to satisfy $|W_2(j\omega)| > |\Delta_m(j\omega)|\ \forall\ \omega$.

Since specification 2 with $|W_{21}(j\omega)| > \Psi\ \forall\ \omega$ is sufficient to achieve specification 1, all three can be unified into a single H_∞ norm-bound criterion. The block diagram for the weighted plant is shown in Figure 4.

The LPV control synthesis can be formulated using LMIs, solvable through convex optimization techniques [20]. This formulation applies to systems with state-space equations in the general form:

$$\begin{aligned} \dot{x} &= A(\kappa)x + B_w(\kappa)w + B_u u \\ z &= C_z(\kappa)x + D_{zw}(\kappa)w + D_{zu}u \\ y &= C_y x + D_{yw}w + D_{yu}u \end{aligned} \tag{5}$$

where the matrices are affine in a parameter κ that varies within a fixed interval. The LPV controller solution (A_c, B_c, C_c, D_c) is similarly parameter-dependent:

$$K_c(\kappa) = [A_c(\kappa), B_c(\kappa), C_c(\kappa), D_c(\kappa)] \tag{6}$$

The controller is synthesized by solving the LMIs for the set of vertex systems, producing vertex controllers to form the parameter-dependent controller matrices. For this problem, the controller can be expressed as:

$$K_c(\kappa) = K_c(\underline{\kappa}) + \alpha\big(K_c(\bar{\kappa}) - K_c(\underline{\kappa})\big) \tag{7}$$

where the scheduled parameter is $\alpha = \big(\kappa - \underline{\kappa}\big)/\big(\bar{\kappa} - \underline{\kappa}\big) \in (0,1)$. Note that α will be the adjustable parameter for the controller.

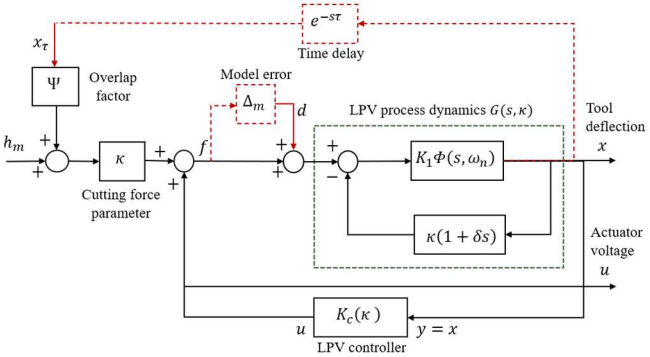

Figure 3. System definition for robust LPV control synthesis.

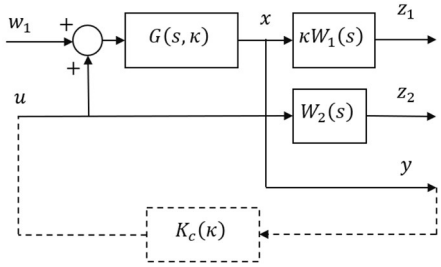

Figure 4. LPV plant definition with weighting functions.

The multiplicative model error (as shown in Figure 5) was calculated based on the error between the single-degree-of-freedom dynamic model (Eq. 1), obtained using the peak picking method for identifying the modal parameters of the first mode, and the FRF results from frequency response testing. Simultaneously, sensitivity calibration was performed around the first resonance frequency, converting from voltage units to meters by matching the piezoelectric bending sensor with the accelerometer data. The results of this stage are presented in Figure 6. The transfer function from the PEA input (in volts) to the PES measurement (in µm) was thus determined as:

$$K_1\Phi(s) = \frac{X(s)}{U(s)} = \frac{K_1}{s^2 + 12s + (2\pi\times 400)^2} \tag{6}$$

where $K_1 = 4.161\ \mu m/\mathrm{Vs}^2$ and $K_2 = 2.575\ \mu m/\mathrm{Ns}^2$. For the tested design case, the maximum value of the force coefficient was set to $\bar{\kappa} = K_2 K_s b \cos\beta / K_1 = 0.22\ \mathrm{V}/\mu m$ (based on $K_s b = (7.5 \times 10^8) \times (1 \times 10^{-3})\ \mathrm{N/m}$ and $\beta = 15°$).

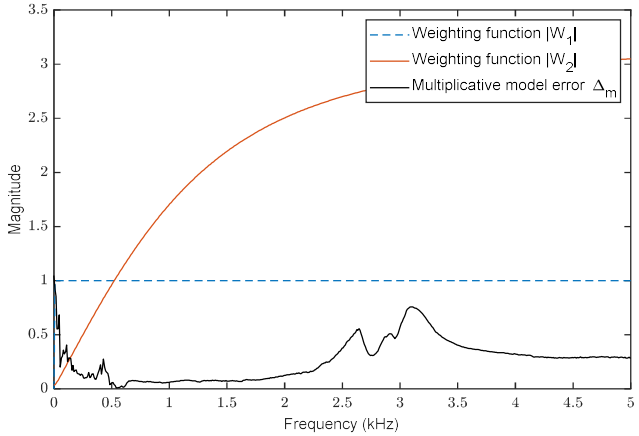

Figure 5. Design weighting functions and model error.

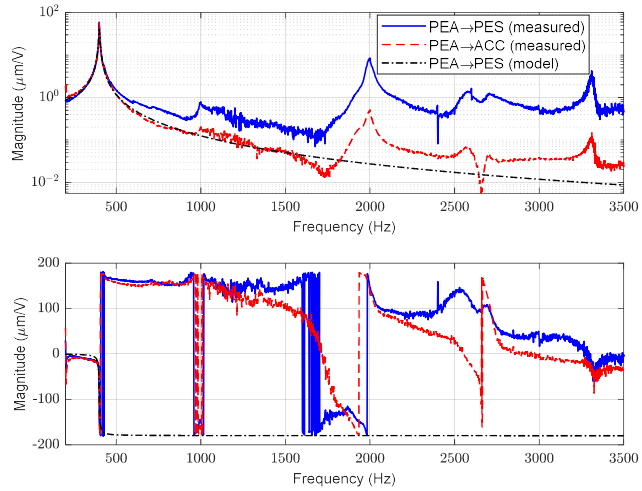

Figure 6. Frequency response measurements from sine-sweep tests with PEA excitation, alongside model-based data for comparison (after tuning).

To align with the robust stability condition outlined in design specification 1 and to reduce the complexity of the synthesis process, $W_1(s)$ was selected as a flat weighting with a unity gain scaling. In contrast, $W_2(s)$ was chosen to bound the model error for $G(s)$, based on the FRF measurement results.

The transfer functions used for robust LPV control synthesis, along with the vertex LPV plant models, are shown in Figure 7. The design results demonstrate that the approach enables real-time tuning of a critical parameter, allowing adjustment of the trade-off between achieving high performance and avoiding excessively large controller gains.

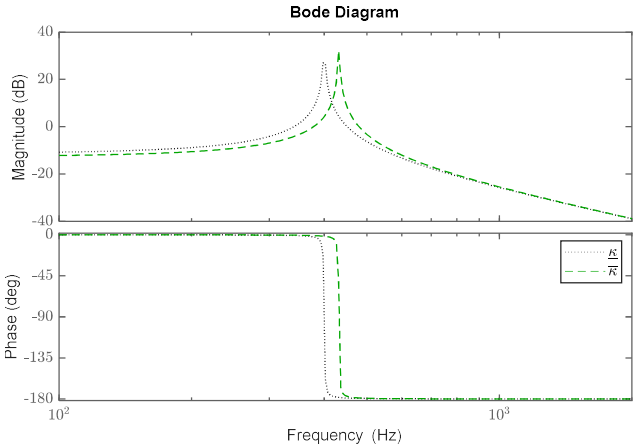

Figure 7. Transfer functions for robust LPV control with vertex plant models.

III. EXPERIMENTAL SYSTEM

The active tool system, shown in Figure 8, was constructed using a commercially available internal turning tool holder (model S32T-MCLNL12 from K. CUTTER), measuring 300 mm in length with a 32 mm diameter. Actuation was achieved through two multilayer piezoceramic stacks (model P-888.31 from PI Ceramic GmbH), each measuring 10 × 10 × 17 mm, with a nominal displacement range of 11 µm and a blocking force of 3500 N. To ensure proper dynamic operation, a preload of 15 MPa was applied via a wedge mechanism with a preload screw. The actuator slots were machined near the clamping area, resulting in an overhang of 180 mm and an L/D ratio of 5.625.

A piezoelectric patch sensor (model P-876.SP1 from Physik Instrumente (PI) GmbH) was installed to measure longitudinal strain, which correlates with radial bending of the tool holder, and was positioned near the actuators. For sensor calibration, an IEPE accelerometer (model CA-YD-1181 from Sinocera) was mounted near the tool insert in the radial direction.

The experiments utilized a cutting force emulator system in a laboratory hardware setup of the tool, as shown in Figure 8. The control block diagram is depicted in Figure 9. The setup included two main real-time subsystems: one for chatter force emulation and the other for active vibration control. Chatter emulation was performed using an electromagnetic actuator powered by an Escon 24/2 amplifier from Maxon Motor, operating in current control mode. The pair of piezoelectric actuators were driven differentially using two piezo amplifiers (model E-617 from PI Ceramic GmbH).

Data acquisition and control were managed using a real-time target machine from Speedgoat, equipped with an IO397 analog input/output card. Both the control algorithm and chatter emulator were implemented in Simulink and MATLAB. A High-Pass Filter (HPF) with a cutoff frequency of 30 Hz was applied to prevent the controller from compensating for quasi-static measurements. Additionally, a real-time user interface enabled online adjustment of controller parameters. The upper part of Figure 9 shows the

chatter emulator, which incorporates chip processing parameters and simulates the chatter force using the electromagnetic force driven by the current amplifier.

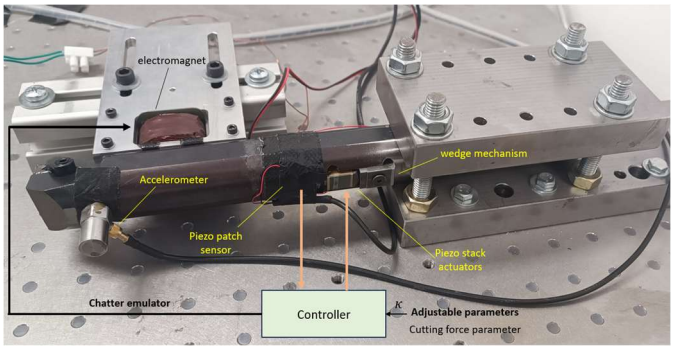

Figure 8. Experimental setup.

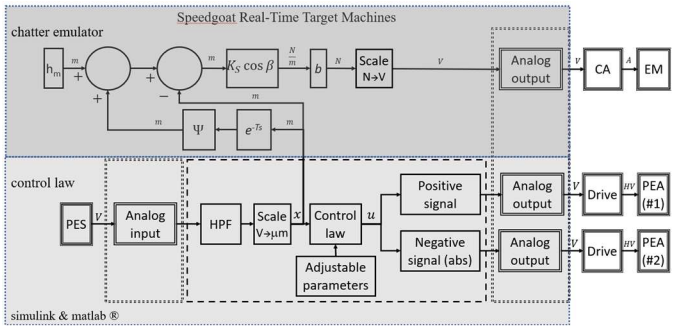

Figure 9. Block diagram of experimental implementation hardware.

IV. Experimental Results

Turning emulation experiments were conducted using the experimental setup (Figure 8). The gain-scheduled H_∞ control law was synthesized using MATLAB. To demonstrate the control effectiveness in a laboratory setting, several key results are presented here. Figure 10 shows the measured FRF of the internal cutting tool for the uncontrolled case, along with three cases using robust LPV control with the two vertex models and one interpolation case. The results support the design and demonstrate that high damping was achieved in the system's resonant frequency range.

Time-domain results from the chatter emulator are shown in Figure 11 for three different cases: Case 1 (red) and Case 2 (black) represent unstable machining conditions without and with control, respectively. Case 3 (blue) represents stable machining parameters without control. Table 1 presents quantitative measures for these cases and an additional Case 4 (without the chatter emulator), which yields results similar to Case 3, thereby confirming the absence of chatter in Case 3. The results show approximately a 65% reduction in chatter vibration (in terms of Root-Mean-Square, RMS value) and about a 47% reduction in the peak value. The value of the dynamic chatter force (f_c) also decreases from Case 1 to Case 2 due to the reduction in the chip thickness parameter (emulated), where PEA is a piezoelectric actuator and PES is a piezoelectric sensor. Quantitative and comparative results with and without control in an internal turning machine were validated in a subsequent study [21], demonstrating improvements consistent with the trends observed here under laboratory conditions with the emulator.

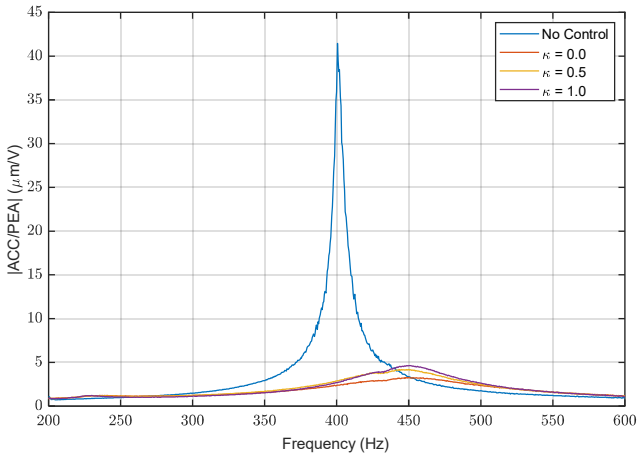

Figure 10. Measured FRF for LPV control with vertex models.

TABLE I. Quantitative Measures

Parameter	*Case 1*	*Case 2*	*Case 3*	*Case 4*	*Units*
PES(rms)	1.82	0.63	0.383	0.379	μm
PES(max)	5.88	3.10	0.910	0.855	μm
f_c (rms)	9.34	2.87	0.157	0.000	N
f_c(max)	29.68	13.77	0.633	0.000	N
Control(rms)	0.00	0.32	0.000	0.000	V
Control(max)	0.00	1.19	0.000	0.000	V

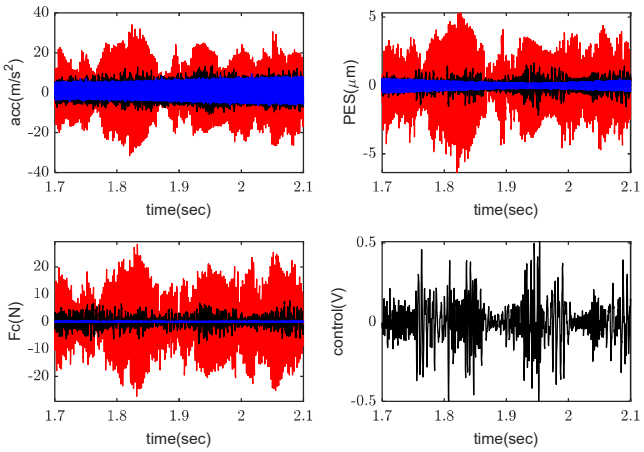

Figure 11. Experimental results for emulator turning: (red) case 1: unstable cutting regime without control, (black) case 2: control applied in unstable cutting regime, (blue) case 3: stable cutting regime withought control.

V. CONCLUSIONS

This study investigated the effectiveness of a robust gain-scheduled H_∞ control strategy for suppressing chatter in internal turning processes. Experimental validation using an emulator setup showed that the proposed controller significantly reduced vibrations in the system's unstable operating region, achieving a reduction of approximately 65% in RMS values and 47% in peak values of chatter forces. These results confirm the practical feasibility of the tunable real-time controller in machining environments, including adaptation to varying cutting conditions.

The research emphasizes the importance of addressing both model uncertainties and time-delayed feedback in controller design. By employing LPV control synthesis with vertex models, the system could maintain robust performance across different machining setups, effectively mitigating instability without compromising operational efficiency

Future work will focus on validating the control design through practical turning experiments in a workshop environment. Additionally, the control algorithm will be extended to more realistic scenarios, such as when the turning tool is connected to CNC machines at varying lengths, causing changes in resonance frequency. This extension will further enhance the adaptability and effectiveness of the control strategy in industrial applications.

ACKNOWLEDGMENT

This research was supported by Israel Innovation Authority Fund 2024, Israel [83647] and by Chiang Mai University Fundamental Fund 2024 [FF041/2567].

REFERENCES

[1] R. Ye, "CNC Machining industry trends," 3ERP, Jun 2019. [Online]. Available from: https://www.3erp.com/blog/cnc-machining-industry-trends-2019 [retrieved: Jan, 2025].

[2] R. P. Siddhpura, "A review of chatter vibration research in turning," International Journal of Machine Tools and Manufacture, vol. 61, pp. 27-47, 2012.

[3] ISCAR, "Anti-vibration boring bars with exchangeable turning heads," [Online]. Available from: https://www.iscar.se/newarticles.aspx/countryid/15/newarticleid/2344 [retrieved: Jan, 2025].

[4] A. Preumont, "Mechatronics: dynamics of electromechanical and piezoelectric systems," Springer Netherlands, Germany, 2006.

[5] Z. Brand and M.O.T. Cole, "Piezo-based flexural vibration suppression for an annular rotor via rotating-frame H2 control optimization,". Journal of Intelligent Material Systems and Structures, vol. 33, no. 4, pp. 572-589, 2022.

[6] Z. Brand and M.O.T. Cole, "Mini-max optimization of actuator/sensor placement for flexural vibration control of a rotating thin-walled cylinder over a range of speeds," Journal of Sound and Vibration, vol 506, p. 116105, 2021.

[7] Y. Wu, Y. Zhang, X. Guo, et al., "Active control of cable vibration using piezoelectric actuators considering strong electric field nonlinearity," Journal of Vibration Engineering and Technologies, vol. 12, pp. 935-947, 2024.

[8] T. Liu, C. Liu, and Z. Zhang, "Adaptive active vibration control for composite laminated plate: Theory and experiments," Mechanical Systems and Signal Processing, vol 206, p. 110876, 2024.

[9] A. Preumont, "Active damping, vibration isolation, and shape control of space structures: A Tutorial," Actuators, vol. 12, p. 122, 2023.

[10] J. Chen, H. Ma, Z. Liu and Z. Liu, "Finite-frequency H_∞ control for active chatter suppression in turning,". International Journal of Advanced Manufacturing Technology, vol. 129, pp. 5075–5088, 2023.

[11] G. Han, H. Ma, Y. Liu, Z. Liu, and Q. Song, "Model-free finite frequency H_∞ control for active chatter suppression in turning," Journal of Sound and Vibration, vol. 577, p. 118342, 2024.

[12] M. Chen and C.R. Knospe, "Control approaches to the suppression of machining chatter using active magnetic bearings," IEEE Transactions on Control Systems Technology, vol. 15, no. 2, pp. 220–232, Mar. 2007.

[13] E. Mizrachi, S. Basovich, and S. Arogeti, "Robust time-delayed H_∞ synthesis for active control of chatter in internal turning," International Journal of Machine Tools and Manufacture, vol. 158, p. 103612, 2020.

[14] M. Kasprowiak, A. Parus, and M. Hoffmann, "Vibration suppression with use of input shaping control in machining," Sensors, vol. 22, p. 2186, 2022.

[15] Y. Altintas and A.A. Ber, "Manufacturing automation: metal cutting mechanics, machine tool vibrations, and CNC design," Applied Mechanics Reviews, vol. 54, no. 5, p. B84, 2001.

[16] T. Schmitz and K. Smith, "Machining dynamics: frequency response to improved productivity," 2nd ed., 2019.

[17] L. Zhang, X. Wang, and S. Liu, "Analysis of dynamic stability in a turning process based on a 2-DOFs model with overlap factor," Journal of Mechanical Science and Technology, vol. 26, no. 6, pp. 1891–1899, 2012.

[18] M. Chen and C.R. Knospe, "Control approaches to the suppression of machining chatter using active magnetic bearings," IEEE Transactions on Control Systems Technology, vol. 15, no. 2, pp. 200–232, 2007.

[19] P. Ruttanatri, M.O.T. Cole, R. Pongvuthithum, and S. Huyanan, "H-infinity controller design for chatter suppression in machining based on integrated cutting and flexible structure model," Automatica, vol. 130, p. 109643, 2021.

[20] S. Boyd, L. El Ghaoui, E. Feron, and V. Balakrishnan, "Linear matrix inequalities in system and control theory," SIAM, 1994.

[21] Z. Brand, M.O.T. Cole, and N. Razoronov, "An active tool holder and robust LPV control design for practical vibration suppression in internal turning," Control Engineering Practice, vol. 156, p. 106215, 2025.